PHYSICAL REVIEW B VOLUME 27, NUMBER 6 15 MARCH 1983

CO chemisorption on Fe(110) studied by angle-resolved photoemission

E. S. Jensen
Cornell Materials Science Center, Cornell University, Ithaca, New York 14853-0161
and Laboratory of Atomic and Solid State Physics, Cornell University, Ithaca, New York 14853-0161

T. N. Rhodin
Cornell Materials Science Center, Cornell University, Ithaca, New York 14853-0161
and School of Applied and Engineering Physics, Cornell University, Ithaca, New York 14853-0161
(Received 16 April 1982)

An angle-resolved ultraviolet photoemission spectroscopy (UPS) investigation of CO chemisorbed on Fe(110) at 200 K is presented. The binding energies at normal emission of the CO 3σ, 4σ, 5σ, and 1π molecular orbitals are determined to be 27, 11.0, 8.3 and 6.8 eV, respectively, at saturation coverage. The 5σ binding energy is coverage dependent, decreasing to 7.6 eV at very low coverage. The identification of the 5σ and 1π peaks is made with the symmetry rules for normal-emission UPS. The variations of the 4σ, 5σ, and 1π peak positions with the parallel component of electronic momentum are extensively investigated. The bandwidths observed are 0.3, 0.8, and <0.3 eV for the 4σ, 5σ, and 1π peaks, respectively, in the [001] mirror-plane direction. In the [1$\bar{1}$0] direction, they are 0.2, 0.5, and <0.3 eV. Both the bandwidths and momentum dependences observed for the 4σ and 5σ peak positions are much more isotropic than can be accounted for by simple band dispersion for the highly anisotropic rectangle implied by the low-energy electron diffraction (LEED) pattern. Accordingly, a more isotropic geometry is proposed that can also be made consistent with the LEED pattern.

I. INTRODUCTION

This paper reports an angle-resolved ultraviolet photoemission spectroscopy (UPS) investigation of CO chemisorbed on (110) surfaces of clean iron single crystals. The results are discussed and compared with the results of previous investigations of CO chemisorption on Fe(110) with the use of other electron spectroscopies and with previous angle-resolved UPS investigations of CO chemisorbed on other transition-metal surfaces. Some of the results have been published previously.[1,2]

Chemisorption refers to the chemical bond formed between an individual atom or molecule and an extended solid surface. This bond is of practical interest because of the wide use of transition-metal surfaces for catalyzing chemical reactions, because its creation is the initial stage in many corrosion processes, and because of the importance of semiconductor surfaces in device fabrication. The CO—transition-metal bond plays a part in the Fischer-Tröpsch catalytic reactions. This practical aspect is one of the motivating factors for the study of CO chemisorption. More importantly, though, CO is a very simple molecule that often retains much of its molecular identity after chemisorption, chemisorbs and desorbs easily and cleanly, and has large cross sections for many surface probes. Thus, independent of any direct applicability in industrial processes, it has served as the prototypical molecular chemisorption system on which many new techniques and new ideas have been tested.

CO in the gas phase is characterized by a 1.13-Å C-O separation, a small dipole moment of 0.112 debye with the carbon end negative,[3] and a dissociation energy of 11.24 eV.[4] There are four valence molecular orbitals. They are known as the 3σ, the 4σ, the 1π and the 5σ molecular orbitals in order of decreasing binding energy. Their ionization energies as measured by UPS are listed in Table I. The 3σ and 1π orbitals are the C—O bonding orbitals. The 4σ orbital is typically thought of as an oxygen lone pair and the 5σ orbital as a carbon lone pair.

The prototypical CO chemisorption system is the $c(2\times2)$CO-Ni(100) system. This system has been extensively studied by numerous surface-sensitive techniques and quite a bit about this system is now known. From electron-energy-loss spectroscopy[5] (EELS) and UPS,[6] the CO is known to be associated. Angle resolved UPS (Ref. 6) and low-energy electron diffraction (LEED) (Refs. 7 and 8) measurements have determined that the CO molecule is chemisorbed with its molecular axis normal to the surface and its carbon end down. The C—O bond length,

TABLE I. CO valence-level binding energies (eV), and CO peak widths (eV) (HWHM).

	Fe(110)[a]			Ni(100)[b]	
	Low coverage	$p(1\times2)$	$c(2\times2)$	Saturation coverage	Free CO
3σ		27.0±1.0			38.5[c,d]
4σ	10.8	11.0±0.1	10.6	10.8	19.7[c,d]
5σ	7.6	8.3±0.2	8.0	8.2	14.0[c,d]
1π	6.8	6.8±0.2	7.5		16.9[c,d]

	Fe(110) $p(1\times2)$[a]	Ni(100) $c(2\times2)$[f]	Free CO
3σ	3.5±0.5		1.0[c]
4σ	0.45±0.1	0.55	<0.1[e]
5σ	0.7±0.1	0.6	<0.1[e]
1π	0.9±0.1	1.0	0.25[e]

[a]This work at normal emission. Peak widths are measured on the high-binding-energy side of the 5σ and on the low-binding-energy side of the 1π.
[b]The $c(2\times2)$ entries are from Ref. 6, while the coverage shifts reported in Ref. 19 (with no reference energy) are added to them to produce the saturation coverage entries.
[c]From Ref. 28.
[d]With respect to the vacuum level.
[e]From Ref. 27.
[f]From Ref. 6.

from LEED, is 1.1±0.1 Å.[7] The UPS peak positions are all broader and shallower than the gas-phase ionization energies. These positions and widths are listed in Table I. An unfortunate consequence of the UPS peak shifts observed for chemisorbed CO is that the most interesting of the CO valence levels, the 5σ and 1π levels, end up nearly degenerate. This fact has made many previous studies of chemisorbed CO difficult to analyze.

There is no realistic calculation that quantitatively describes the interaction of a CO molecule with any transition-metal surface. The most relevant existing calculations are for hypothetical metal-CO molecules.[9–12] The relevant results of these calculations are easily summarized. The 3σ, 4σ, and 1π levels are found to be changed very little from the gas phase. The main metal—CO bond is formed by the 5σ level, and the resulting bonding level is moved to deeper binding energy. The charge transfer involved in this bond is compensated by the creation of another CO-metal hybrid level whose CO component is the 2π level, unoccupied in gas phase. The 2π orbital is antibonding with respect to the C—O bond.

This model does not itself explain the observed shift of all binding energies toward the vacuum level. This effect is explained as a failure of UPS to measure simple one-electron binding energies. Even though the initial state involved can be thought of as relatively unperturbed, the hole left behind after photoemission is better screened by the coordinated CO ion than by the free CO ion, so that the observed photoelectron will have higher kinetic energy and less apparent binding energy. References 9 and 13 attempt to describe the screened state in some detail.

CO chemisorption on iron has not been extensively studied and is qualitatively different from CO chemisorption on the more commonly studied substrates of nickel, copper, palladium, and others. At room temperature on Fe(110), the adsorbed CO slowly dissociates,[14] while it is quite stable on most other substrates. The dissociation can be avoided by adsorbing the CO at temperatures below 300 K.[1] One might expect this tendency towards dissociation, evidence of a weakened C—O bond, to appear in the UPS spectrum as different CO orbital binding energies. The four CO valence-level binding energies for the CO-Fe(110) system are reported in Sec. III. They are found to differ in one significant respect from the binding energies of CO chemisorbed on other substrates. The position of the 1π-derived level is a full eV shallower than it is in the prototypical $c(2\times2)$CO-Ni(100) system.[6] This difference is qualitatively predicted for an unstable molecule by a simple model due to Brodén *et al.*[15]

The UPS results turn out to have significance beyond their potential indication of an unstable molecule. This interest stems from the fact that the traditional CO chemisorption systems are rather unsatisfactory systems for study by UPS. The problem is that the two most interesting CO-derived levels (the "-derived" will hereafter be suppressed), the 1π

and 5σ molecular orbitals, are nearly degenerate in energy for chemisorbed CO. In the $c(2\times2)$CO-Ni(100) system, they are separated by 0.5 eV with the 1π peak at a shallower binding energy.[6] The peaks themselves have intrinsic widths of about 1 eV halfwidth at half maximum (HWHM), and are not resolved. On Fe(110) at low temperatures, the 1π level is shifted by another electron volt, yielding a total separation of 1.5 eV. Because of this binding-energy separation the relative cross sections for photoionization versus photon energy can be easily measured. These data are also reported in Sec. III. They are compared to calculations for gas-phase-oriented CO molecules,[16] and exhibit surprisingly good qualitative agreement.

Another series of measurements was made possible by the relatively large binding-energy separation of the 1π and 5σ peaks. These orbitals have the largest spatial extent of the four valence levels of the gas-phase molecule. For the CO density observed on Fe(110), nearest-neighbor 5σ and 1π orbitals are expected to overlap one another and form two-dimensional bands with bandwidths of about 1 eV.[17] Angle-resolved UPS permits a direct observation of the variation of these binding energies with momentum. This is a standard application of angle-resolved UPS, first made on a chemisorption system by Larsen *et al.*[18] Other measurements of two-dimensional band formation for chemisorbed CO have proved difficult to interpret because of the small binding-energy separation between the 5σ and 1π peaks, and because of the complex geometries involved.[17,19–22] Two-dimensional band-dispersion data for CO adsorbed on Fe(110), in which the individual contributions of the 1π and 5σ levels are clearly distinguished, are presented in Sec. V.

The geometry inferred from the LEED pattern alone is a simple anisotropic rectangle. It was expected that measurements of the bandwidths in the two quite different mirror-plane directions would reflect this anisotropy and provide detailed information about the spatial extent of the CO molecular orbitals. This expectation proved incorrect. Both the bandwidths and the momentum dependences of the binding energies appear quite isotropic. These observations lead to the proposal of a new, more isotropic geometry in Sec. V.

II. EXPERIMENTAL APPARATUS AND SAMPLE PREPARATION

Data were taken at the Synchrotron Radiation Center of the University of Wisconsin in Stoughton, Wisconsin. The spectrometer consists of a two-level ion-pumped μ-metal ultrahigh-vacuum chamber. The upper level is used for sample cleaning and characterization while the lower level lets in the synchrotron radiation and contains the angle-resolving analyzer. The analyzer is a hemispherical electrostatic analyzer made by Vacuum Generators (VG) (Model ADES400) mounted on the standard VG goniometer. Typical operating parameters are of 15-eV pass energy and a 10-eV sweep into 512 channels repeated 10 times with a dwell per channel of 0.1 sec. Typical analyzer contribution to the overall resolution is 0.2—0.3 eV. For all data reported the analyzer was kept within the horizontal plane, which is also the plane of polarization. The analyzer can approach within 15° of the light beam. The angle-resolved UPS geometry is shown schematically in Fig. 1. Vacuum is typically $(1-2)\times10^{-10}$ Torr during UPS measurements. All spectra shown have been digitally smoothed.

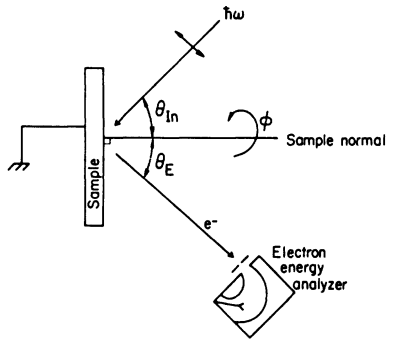

FIG. 1. Schematic geometry for angle-resolved UPS. Up is out of the page. Variable parameters are the photon energy ($\hbar\omega$), the sample azimuth (ϕ), the incidence angle (θ_{in}), and the electron exit angle (θ_E). θ_E is positive as shown and denoted negative if on the same side of the sample normal as the light beam.

On the upper level there are facilities for LEED, Auger electron spectroscopy (AES), argon-ion sputtering, and mass spectrometry. The sample is moved from probe to probe by a vertically mounted sample manipulator. This manipulator provides lateral motion and rotation about the vertical axis. The sample can also rotate about its normal. The sample holder was specially adapted for liquid-nitrogen cooling and the sample reaches about 80 K. The temperature is measured with a chromel-alumel thermocouple spot-welded to the rear corner of the sample. The sample is heated by electron bombardment from a tungsten filament located directly behind the sample. Typical heating parameters are 10 mA at 500 eV.

The Fe(110) samples were oriented with x-ray diffraction to within 1° of (110) and mechanically polished with alumina grit down to a grit size of 0.05 μm. A typical polished sample was $1.0\times0.5\times0.05$ cm^3.

Initial AES spectra typically indicated large quantities of sulfur, carbon, and oxygen. Initial cleaning required weeks. The samples were argon-ion sputtered for long periods of time (for hours at 500-eV argon energy with about 20 μA on the $\frac{1}{2}$-cm^2 face) alternately hot (700 °C) and cold (room temperature). This process was continued until a 700 °C flash did not move observable quantities of contaminant to the surface. Carbon would sometimes seem invulnerable to sputtering. This problem could be attacked by 300—400 °C treatments in 10^{-7} Torr of hydrogen or oxygen. A final cleaning before taking data was usually a 5-min sputter followed by a flash to 600 °C. Traces of carbon, oxygen, and nitrogen are evident and estimated to be in the 1-at. % contamination range.

The sample was then cooled, reflashed, and examined with LEED. If a good 1×1 pattern was observed, the sample was lowered to the UPS level, reflashed, and exposed to CO. The 1×2 pattern was typically produced by a 100-sec exposure to 3×10^{-8} Torr of CO (uncorrected gauge reading). Sometimes AES indicated a clean sample, but the LEED pattern exhibited faint 2×2 spots. Several 600 °C flashes would typically remove the 2×2 spots and yield a good quality 1×1 pattern. It is assumed that the flashes drive traces of contaminant into the bulk where they are trapped by the rapid cooldown.

The LEED pattern for the CO-covered substrate was examined subsequent to the data collection, to avoid electron-beam damage. Damage was commonly visible in about a minute with a 100-eV, 5-μA beam.

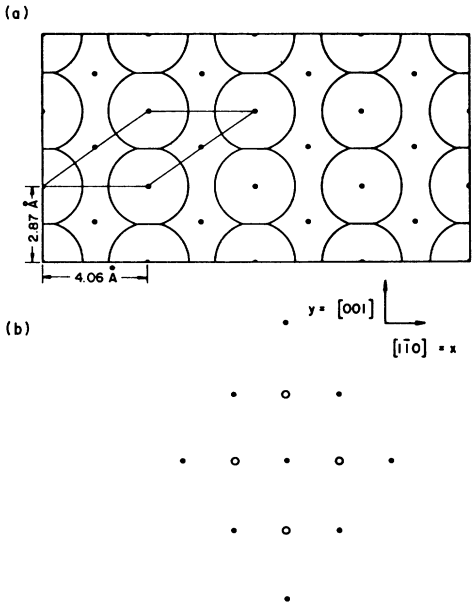

FIG. 2. (a) $p(1\times2)$CO-Fe(110) geometry. Dots are the Fe atoms and the circles represent CO molecules. (b) Schematic $p(1\times2)$CO-Fe(110) LEED pattern. Dots are the primary spots and the circles represent the extra (1×2) spots.

III. REVIEW OF PREVIOUS STUDIES

The angle-integrated UPS investigation of Brodén *et al.*[14] first noted that this surface slowly dissociates the CO molecule at 300 K. Subsequent investigations have determined that this dissociation does not occur at temperatures near or below 200 K.[1,23] The work-function change increases smoothly to a maximum change of 0.86 eV after an exposure of 0.5 L (1 L = 1 langmuir = 10^{-6} Torr sec).[23]

The saturation coverage LEED pattern observed is shown in Fig. 2 along with its most straightforward transformation to real space. The CO molecules are portrayed as circles of radius 3.1 Å to indicate the 10^{15}-CO/cm^2 density typically observed for low-temperature saturation adsorption of CO. This structure is called $P(1\times2)$ and the unit cell that gives rise to this name is also indicated in Fig. 3. The coverage is $\frac{1}{2}$ monolayer, and the CO density is 0.89×10^{15} CO/cm^2. Observations were made at both 80 and 200 K with no observably different behavior. The pattern develops as streaks in the [001] direction that coalesce to somewhat diffuse spots after an exposure of about 1.5 L. The spots are of moderate quality and are slightly less sharp than the original primary spots and those observed

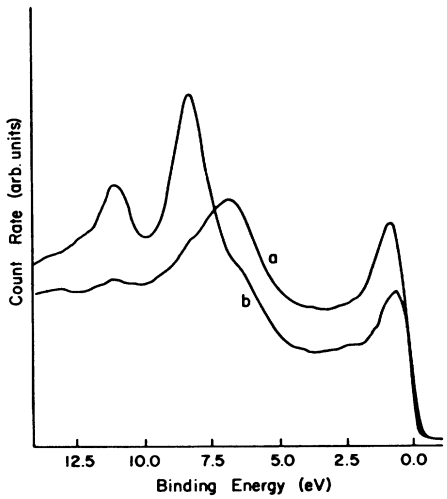

FIG. 3. Normal-emission UPS spectra illustrating the shift in binding energy of the 1π-5σ doublet. Curve *a* is taken with a 21-eV photon energy at a 20° angle of incidence. Curve *b* is taken at 28 eV, 45°.

for the sequence of LEED patterns for CO chemisorption on Ir(111).[21] The second-order overlayer spots are dimly visible with a primary energy of 205 eV. Peaks in the intensity of the first-order overlayer spots occur at primary energies of about 75, 115, and 205 eV.

Subsequent LEED observations by Erley[23] have resolved a distinct $\frac{1}{4}$ monolayer structure called $c(2\times4)$. This structure is shown in Fig. 2. Electron-loss spectroscopy (ELS) measurements by Erley have determined that the CO stretch energy is 246 meV and that the CO-Fe stretch energy is 55 meV, both at saturation coverage. Erley also reports an unexpected ELS peak at 45 meV that he attributes to a frustrated rotation of the CO molecule. Observation of this mode with ELS requires an asymmetric adsorption site. Erley proposes that the simple rectangle implied by the LEED pattern alone is slightly distorted to produce this asymmetric binding site.

IV. NORMAL EMISSION UPS RESULTS AND DISCUSSION

Normal emission spectra for the $p(1\times2)$CO-Fe(110) system at photon energies of 21 and 28 eV are presented in Fig. 3. The shallower peak shifts 1.5 eV from 6.8 to 8.3 eV as the photon energy is raised from 21 to 28 eV. This shift is explained as a 1.5-eV separation in binding energy between the 1π and 5σ peaks and a strong variation in relative cross section with photon energy.

The symmetry selection rules first discussed and applied by Jacobi *et al.*[24] are used to identify the 1π and 5σ contributions. These rules require that with p-polarized light σ emission disappears as θ_{in} (Fig. 1) approaches zero, while π emission maximizes there. Their application is shown in Fig. 4 as plots of total peak area versus angle of incidence at three different photon energies. For 23-eV photon energy the peak is at 6.8 eV and a nonvanishing intensity is observed as the angle of incidence approaches zero. For 27-eV photon energy the peak is at 8.3 eV and the intensity of emission clearly disappears as normal incidence is approached. The symmetry rules thus require that the 6.8-eV components have π symmetry, and that the 8.3-eV components have σ symmetry.

Figure 5 is an energy-distribution curve (EDC) taken with a photon energy of 90 eV, and indicates a fourth CO-derived peak at a binding energy of 27 eV. This peak is identified as emission from the CO 3σ level. The binding energies and peak widths of all four valence levels are tabulated in Table I.

Since the 5σ and 1π peaks are now nearly resolved they are easy to follow versus photon energy. The strong variation in cross section observed in

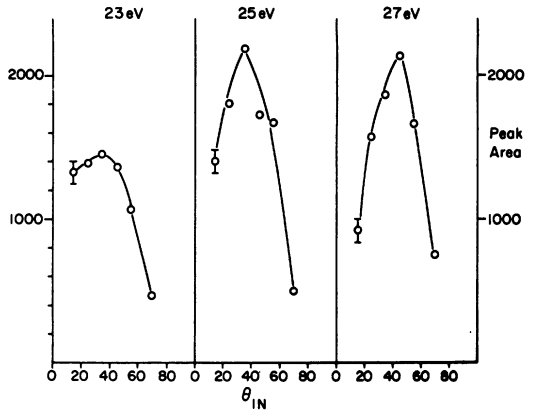

FIG. 4. Total area of lower-binding-energy peak (5σ and 1π) at normal emission vs incidence angle for photon energies of 23, 25, and 27 eV. Indicated uncertainty applies to all points and the solid line is merely a guide.

Fig. 3 is quantified and extended to higher photon energies in Fig. 6. Relative cross sections at 45° angle of incidence versus photon energy from 21 to 48 eV are presented for the 1π, 5σ, and 4σ peaks. For the (21–26)-eV photon-energy range, where significant 1π emission is seen, the single peak seen is deconvoluted into 8.3- and 6.8-eV contributions with halfwidths of 0.7 and 0.9 eV, respectively. For higher photon energies the bars shown indicate 20% of the 5σ area and represent the maximum unobservable 1π area. The data presented are normalized to the total photocurrent from a tungsten diode in the light path. Its efficiency has not been divided out. The efficiency is known to be a smooth function of photon energy from 20 to 40 eV and some-

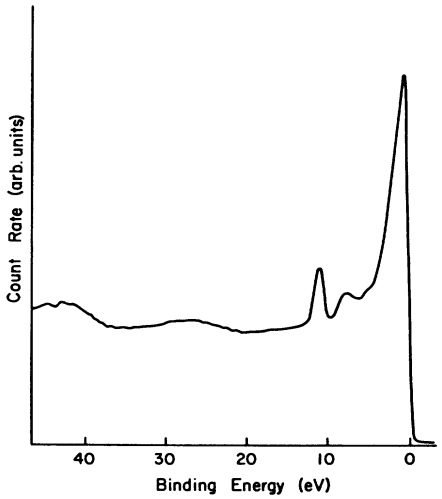

FIG. 5. Spectrum illustrating the CO 3σ peak at 27-eV binding energy. Photon energy is 90 eV, the angle of incidence is 45°, and the electron exit angle is 30°.

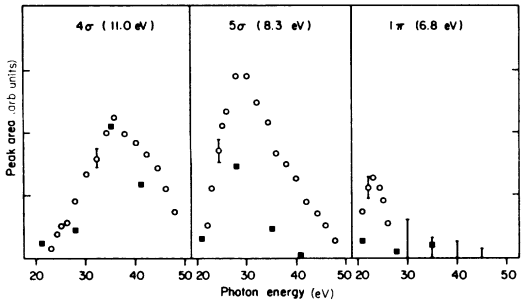

FIG. 6. Normal-emission peak areas vs photon energy for the 4σ, 5σ, and 1π peaks. Circles are the data normalized to a tungsten photodiode (see text) and the filled squares are from a calculation for uncoordinated CO by Davenport (Ref. 16) normalized to the data at the 4σ, 35-eV point. No 1π emission is seen for photon energies above 26 eV and the bars shown represent the maximum unobservable level of 20% of the 5σ area. Angle of incidence is 45°.

what more efficient at 20 eV.[25] The efficiency has not been measured above 40 eV.

Calculated points from Davenport[16] are also presented in Fig. 6. This calculation was for gas-phase-oriented CO molecules. The calculated points are normalized to the data at the 4σ, 35-eV point. The calculations predict behavior qualitatively similar to that observed. The 1π emission is predicted and observed to be most intense at low photon energies. The 4σ and 5σ intensities peak sharply near 36 and 29 eV, respectively, as predicted. The 4σ, 36-eV peak is common to CO chemisorption on Ni(100),[6] Cu(100),[26] and Ir(111),[21] and is attributed to a shape resonance or large final-state amplitude near the molecule. The 5σ peak position is coverage dependent. It is found at 7.6 eV at low coverage and smoothly increases to its 8.3-eV saturation value. The 4σ peak shifts 0.2 eV to deeper binding energy as coverage is increased, and the 1π peak position remains fairly constant. The binding energies at both limits of coverage are presented in Table I. These shifts with coverage track the shifts with exit angle quite well and are attributed to lateral interactions between adjacent molecules.

The fact that the 4σ and 5σ peaks obey the appropriate symmetry rules (their emission intensities disappear as the incidence angle approaches zero) is qualitative evidence for the normal orientation of the CO molecule. These rules would not apply for a tilted molecule. The agreement between the normal emission cross sections seen and those calculated by Davenport[16] for emission along the C-O axis is fur-

TABLE II. CO bandwidths (eV). (a) Predictions for the $p(1\times2)$ CO-Fe(110) system, (b) observations for the saturated CO-Fe(110) system, and (c) previous experimental results ("sat" refers to saturation coverage).

	(a) $[1\bar{1}0]$	[001]
4σ	0.03	0.20
5σ	0.13	0.70
$1\pi_x$	0.27	$\ll$0.85
$1\pi_y$	$\ll$0.27	0.85

	(b) $[1\bar{1}0]$	[001]
4σ	0.2–0.3	0.3–0.4
5σ	0.4–0.6	0.6–0.9
$1\pi_x$	$<$0.3	
$1\pi_y$		$<$0.3

	(c)					
	CO(0001)[a]	Ir(111)[b]		Pd(100)[c]	Ni(100)[d]	
	sat.	sat. $\sqrt{3}\times\sqrt{3}$		sat.	sat. $c(2\times2)$	
4σ	0.45	0.4	0.2	0.4	0.3	0.15
5σ	0.8	0.7	0.3			
1π		$<$0.3	$<$0.3			

[a]From Ref. 22.
[b]From Ref. 21.
[c]From Ref. 20.
[d]From Ref. 19.

ther evidence. In particular, the intensity of the 4σ peak as a function of photon energy of the 4σ level is nearly identical to that reported for the $c(2\times2)$CO-Ni(100) (Ref. 6) system where the molecular orientation has been determined to be normal. Although not proved conclusively, normal orientation of the CO molecule will hereafter be assumed.

C_2V symmetry splits the $1\pi_x$ and $1\pi_y$ levels. The symmetry rules forbid normal emission from the $1\pi_x$ level with the surface component of $A(A_s)$ in the [001] direction, and from the $1\pi_y$ level with A_s in the $[1\bar{1}0]$ direction. Thus a simple rotation of the sample permits tuning from the $1\pi_y$ ([001] horizontal) to the $1\pi_x$ ($[1\bar{1}0]$ horizontal). Normal-emission spectra for the latter geometry are presented in Fig. 7. The splitting is less than 0.3 eV. Dispersion for the $1\pi_y$ peak in [001] is essentially similar.

A most interesting result of the normal-emission UPS study is the 1.5-eV binding-energy separation between the 1π and the 5σ peaks. The other interesting characteristic of the CO-Fe(110) system is its tendency to dissociate CO molecules. It seems reasonable to attempt to relate these characteristics. Such an attempt was made by Brodén *et al.*[15] in 1976, well before these binding energies were measured. They noted that in calculations of the free-CO peak positions[12] the 1π binding energy was quite sensitive to the assumed CO bond distance, shifting about 1 eV for every 0.1-Å stretch (shallower binding energy corresponds to a stretched molecule). The binding energy of the 4σ level, a nonbonding orbital, is relatively insensitive to such a stretch and both orbitals have relatively little direct interaction with the metal. Brodén *et al.* therefore suggested that the 4σ-1π binding-energy separation should be a sensitive indication of the CO bond length and insensitive to the details of the bonding. A large 4σ-1π binding-energy separation indicates a large CO bond length and therefore a molecule that is ready to dissociate. For CO adsorbed on Fe(110) this parameter varies with coverage from 4.0 to 4.2 eV, while it is 3.1 eV in the $c(2\times2)$CO-Ni(100) system[6] and 2.8 eV in gas-phase CO.[27] The model then implies a 0.12-Å stretch in going from the gas-phase to the low-coverage CO-Fe system. It should be noted that the shallow 3σ binding energy is consistent with this interpretation. The 3σ is another C—O bonding orbital and should also be sensitive to the C—O bond length. Bagus *et al.*[9] predict that the 3σ-4σ binding-energy separation shifts 1.6 eV for every 0.1-Å stretch. The 16-eV 3σ-4σ separation observed on Fe(110) is 2.8 eV less than the 18.8-eV gas-phase value.[28] This then corresponds to a 0.18-Å stretch, in surprisingly good agreement with the 0.12—0.14 Å derived from the 1π position. Arguments involving the 3σ level should be considered skeptically because this level is an inner core (a hole in the 3σ is energetically capable of autoionization) even for uncoordinated CO, and extensive shakeup structure accompanies its photoionization peak.[28]

This is a simple model that ignores all other possible contributions to the binding-energy separation of the 1π and 4σ levels. Nevertheless, it is an interesting speculation that is consistent with the observed room-temperature dissociation. There is no direct evidence that CO dissociation on Fe(110) is actually preceded by a stretched CO molecule.

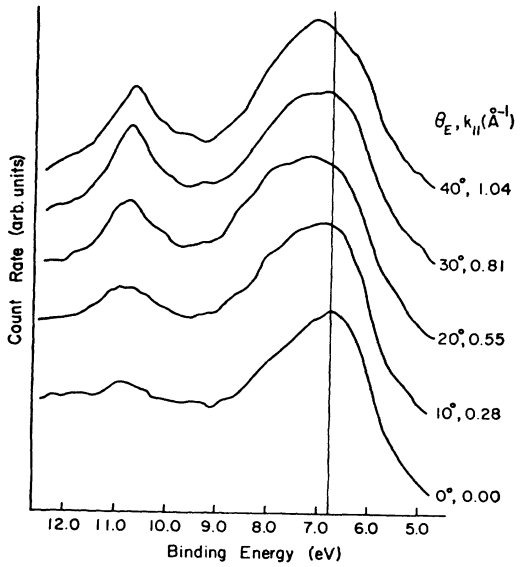

FIG. 7. Dispersion of the $1\pi_x$ peak. Photon energy is 22 eV, the angle of incidence is 15°, and the surface component of polarization is in the $[1\bar{1}0]$ azimuth. Dispersion for the $1\pi_y$ peak in the [001] direction is essentially similar for the corresponding conditions.

V. THE UPS PEAK POSITIONS AS FUNCTIONS OF THE SURFACE COMPONENT OF MOMENTUM

The peak positions observed at normal emission are sensitive functions of the electron exit angle. This is a well-known effect, first observed in an adsorption system by Larsen *et al.*[18] in 1978 and explained as a variation in initial-state binding energy with momentum, followed by conservation of the surface component of momentum ($\vec{K}_s$) in the photoemission process.

CO—transition-metal chemisorption systems have been moderately popular subjects for investigation by this technique. When this study was begun, Ni(100) (Ref. 19) and Pd(100) (Refs. 17 and 20) substrates had been studied. Very little dispersion was

observed for the low-density structures and about 0.3-eV bandwidths were observed for the 4σ and 5σ-1π peaks in the high-density layers. These systems have complex geometries and almost no binding-energy separation between the 5σ and 1π peaks at normal emission. The $p(1\times2)$CO-Fe(110) system seemed to present an opportunity to study the bands formed for a simple geometry with a relatively large separation between the 5σ and 1π peaks. Subsequent to the start of this investigation two other studies have been reported, one on Ir(111) (Ref. 21) and one on Co(0001).[22] Bandwidths of 0.8 eV for the 5σ bands were reported in the dense-packed phases and no 1π peak motion was reported.

Theoretical predictions for these systems are at a very primitive stage. The only published theoretical study accompanied the Pd(100) experimental investigation.[17] This was a tight-binding calculation of the bands formed by the 5σ, 1π, and 4σ levels for an isolated CO layer (no substrate interaction included) for the geometries observed on Pd(100). Since this calculation was for an isolated overlayer, it can be equally well applied to predict the bandwidths for CO adsorbed on Fe(110). The two mirror-plane directions of the rectangular $p(1\times2)$ overlayer are completely independent essentially one-dimensional problems, but with quite different CO-CO spacings. These spacings are 2.87 Å in [001] and 4.06 Å in the [1$\bar{1}$0] direction. These distances correspond well with the CO-CO distances in two of the Pd(100) overlayers for which the calculations were done. Thus, except for the reduced coordination of the one-dimensional problems, the palladium bandwidths should be directly applicable to the iron system. The bandwidths calculated by Batra *et al.*[17] for the two nearly hexagonal CO-Pd(100) systems have been divided by two and listed in Table II as the initial qualitative predictions of the bandwidths in the two mirror-plane directions for the $p(1\times2)$CO-Fe(110) system. One poor characteristic of the calculation is the fact that 5σ-1π hybridization is not included. In the isolated overlayer, the 5σ and 1π binding energies are well separated, so that it is reasonable to ignore this hybridization. However, in the chemisorbed phase the 1π and 5σ binding energies are typically similar and 1π-5σ hybridization could potentially be important. In addition to changing the band structure, hybridization confuses the nomenclature. In this paper the phrase "5σ band" refers to the contiguous band that has σ symmetry at $K_s=0$. Corresponding identifications are made for the 1π bands.

The results are presented below. These data will be seen to disagree with the predicted behavior rather significantly. In particular, the bandwidths and momentum dependences observed are much more isotropic than expected. These differences motivate the proposal of a new geometry that can be made consistent with both the LEED and UPS data.

Dispersion data are presented in Figs. 7 and 8. Figure 7 presents data that are thought to be essentially 1π peak motion, while Fig. 8 presents 4σ and 5σ data. The separation of the 1π and 5σ peak motion is made surprisingly easy because (1) the two bands remain well separated in binding energy (the 1π bands do not disperse), and (2) low [(20—22)-eV] photon energies seem to enhance the 1π emission, while all spectra taken between 28 and 45 eV include no significant emission in the small binding-energy range of the 1π.

Point (1) is made in Fig. 7. These are 22-eV photon-energy spectra taken at a 15° angle of incidence. A peak that remains shallower than about 7.1 eV for all K_s less than about 1 Å^{-1} in each azimuth is identified as a nondispersive 1π band, $1\pi_x$ in [1$\bar{1}$0], and $1\pi_y$ in [001]. The motion seen in Figs. 8 and 9, about 0.3 eV, is an upper limit on the 1π bandwidths. The broadening and shift of approximately 0.5 eV seen for small K_s (0.3—0.7 Å^{-1}) is interpreted as 5σ emission, because the peak narrows and returns toward 6.8 eV as K_s is again increased to about 1.0 Å^{-1}. Other spectra in the (0.3—0.7)-Å^{-1} range encourage this interpretation.

Once it is known that the 1π bands remain near 7 eV, any spectrum that has a small weight near 7 eV can have its peak position associated with the 5σ band. This characteristic is seemingly shared by all spectra taken at 45° angle of incidence between 28-

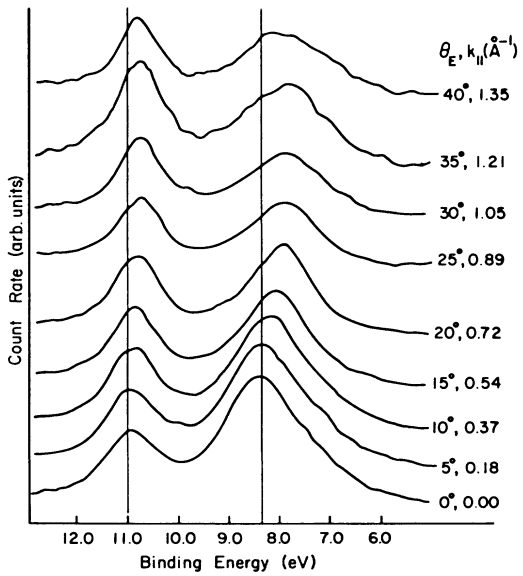

FIG. 8. Dispersion of the 4σ and 5σ peaks in the [1$\bar{1}$0] direction. Photon energy is 32 eV and the angle of incidence is 45°.

and 45-eV photon energy. Figure 8 presents 32-eV spectra for the [1$\bar{1}$0] azimuth. There is evidence of 4σ peak motion in this figure also.

Figure 9 presents a reduced version of Figs. 7 and 8. The 1π results simply report the lack of peak motion observed. The 4σ and 5σ results are the peak positions of spectra taken at 45° angle of incidence averaged over 0.1-Å^{-1} windows for photon energies between 28 and 45 eV. The uncertainty illustrated is the root-mean-square deviation of the approximately 150 spectra which were analyzed. Owing to imprecisions in monochromator calibration these data are all referenced to the 4σ peak position at normal emission (11 eV). The 4σ motion obtained from these data, together with those of another data set taken with a photon energy of 70 eV, are represented on an expanded scale in Fig. 9.

Data were obtained from two samples. The σ-band data presented in Fig. 8 are all from sample 1. The reduced results for the π bands are from both samples (no significant peak motion was observed). The spectra of Fig. 7 is from sample 2.

The behavior observed on the two samples was quite similar, but not identical. The 5σ bandwidth observed from sample 1 (0.8 eV) was consistently larger than that observed from sample 2 (0.6 eV). There were no observable differences in the band shapes or in the behavior of the other bands. The LEED patterns observed from the two samples were not distinguishable by eye. Sample 1 was usually marginally cleaner. Sample 2 had slightly larger amounts of oxygen and nitrogen, although all contaminant levels are small (estimated at about 1—2 at.% from Auger electron spectroscopy). The 5σ orbital, according to the simple chemisorption model presented in Sec. III, is the metal-bonding orbital and might be expected to be sensitive to traces of contamination. No systematic investigation of the dependence of the 5σ bandwidth on surface cleanliness was undertaken.

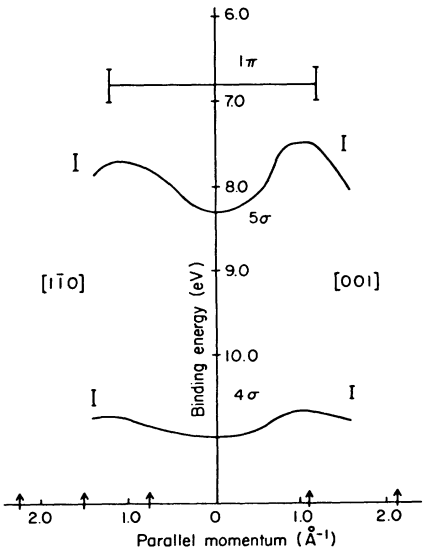

FIG. 9. CO peak motion vs the surface component of momentum. 1π results are from spectra taken with 20-, 21-, and 22-eV photon energies at 15° and 20° angles of incidence. 4σ and 5σ results are the peak position averaged over 0.1-Å^{-1} windows for photon energies from 28—45 eV at a 45° angle of incidence.

Good agreement between observation and expectation is seen for the 4σ and 5σ bands in [001]. The 0.3- and 0.8-eV bandwidths seen are in good agreement with CO band-formation studies on Ir(111) (Ref. 21) and Co(0001).[22]

The data have three characteristics that are difficult to reconcile with the calculation and with the assumed geometry. The first such characteristic is the apparent lack of 1π dispersion. The second is the relatively large bandwidths observed in the [1$\bar{1}$0] direction for the 4σ and 5σ binding energies. The third surprising characteristic is the momentum dependences of the σ bands in [1$\bar{1}$0] direction.

The 1π_y band in the [001] direction is expected to have a bandwidth about as large as the 5σ band (nearly an eV). No significant dispersion is observed. One possible explanation of the lack of 1π dispersion is that the simple model is inappropriate and that substrate interactions have somehow reduced the spatial extent of the 1π orbital. This would have the effect of reducing the observed bandwidths. None of the other four investigations of CO band formation[17,19–22] reported significant dispersion in the 1π band.

The 0.8- and 0.3-eV σ bandwidths in [001] are about as large as expected. A factor-of-6 reduction

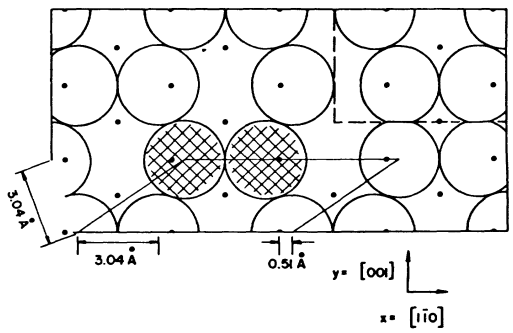

FIG. 10. Proposed distortion of the $p(1\times2)$ into a 2×2 geometry. Dots are the Fe atoms and the circles represent CO molecules. Solid line indicates a unit cell with the hatched basis. Dashed line in the upper right is a wall between two equivalent translational domains.

in 4σ and 5σ bandwidths was predicted upon changing from the [001] to the [1$\bar{1}$0] azimuths. A ratio of about $\frac{3}{2}$ is seen. The large relative bandwidths of the 4σ and 5σ bands in the [1$\bar{1}$0] direction might perhaps be caused by changes in the orbitals due to their metal interactions. This would be a reasonable conclusion for the 5σ band. The 4σ level is not expected to change significantly upon chemisorption, so that an effect as large as that for the 5σ band is unlikely.

The observed momentum dependences of the σ bands in [1$\bar{1}$0] are the most significant (i.e., most difficult to explain) disagreement between expectation and observation. The Brillouin-zone boundaries for the $p(1\times2)$ rectangle are included in Fig. 9 as arrows on the momentum axis at integral multiples of 0.77 Å^{-1}. A simple isolated tight-binding formalism with nearest-neighbor interactions predicts a cosine band shape with a period of 1.54 Å^{-1}. This precise shape is dependent on the model, but the periodicity and the occurrence of zero slope at each zone boundary are model-independent requirements of the geometry. These requirements are clearly not met by the observed peak motion and one is forced to conclude that this peak motion cannot represent simple band dispersion for the assumed geometry.

The observed peak motion does, however, have zero slope at about 1.1 Å^{-1} in the [1$\bar{1}$0] direction. If this flatness were taken to represent a simple zone boundary, then it would correspond to a CO-CO spacing of about 3 Å. Similarly, the large observed amplitudes are suggestive of a CO-CO spacing significantly smaller than that implied by the LEED pattern alone. These observations begin to suggest the existence of a much more isotropic geometry than the 2.87×4.06-Å rectangle.

There are other problems with acceptance of the simple rectangular geometry. The ELS measurements of Erley[23] revealed an unexpected peak at 45 meV that Erley attributed to a frustrated rotation of the CO molecule. The observation of this mode with ELS requires a low-symmetry binding site. Erley also pointed out that the 2.87-Å CO-CO spacing in the [001] direction is significantly smaller than the 3.1—3.2 Å observed as saturation coverage CO-CO spacings in many other CO—transition-metal systems.

All of these observations suggest that the simplest interpretation of the LEED pattern is perhaps inadequate and should be modified. Erley suggested one such modification.[23] It does not, however, explain the photoemission data. The structure illustrated in Fig. 10 is therefore proposed as the saturation-coverage CO-Fe(110) geometry. It results easily from the undistorted $p(1\times2)$ rectangle by a 0.51-Å translation of the CO molecules. The domain wall in the upper right-hand corner of the figure will be considered below.

In this structure, the 2.87-Å spacing has been increased to 3.04 Å and the CO molecule has the low-symmetry site required for observation of the 45-meV vibrational mode. At the same time, the 4.06-Å spacing in the [1$\bar{1}$0] direction has been reduced to 3.04 Å, making the overall geometry much more isotropic. It will be shown below that this modification can explain the UPS data.

One serious problem with this distorted geometry is that it is no longer consistent with the LEED pattern observed. The unit cell is now twice as big as that of the unperturbed geometry, and should be called a 2×2 overlayer. Neither Erley[23] nor we observe any 2×2 spots in the LEED pattern. One might first think that the distortion is small, so that the spots generated by this distortion should be weak. This is incorrect. A straightforward calculation of the structure factor for this geometry predicts that some of the unobserved spots should be as intense as the observed 1×2 spots. The 2×2 spots are generated by the perfect order of the distortion. The absence of 2×2 spots can thus be explained as a lack of long-range order in this distortion. The domain wall illustrated in Fig. 10 is an example of this sort of disorder. Its existence creates domains of 2×2 structure within a long-range-ordered 1×2 overlayer. In the presence of domain walls of this sort the 2×2 spots would be

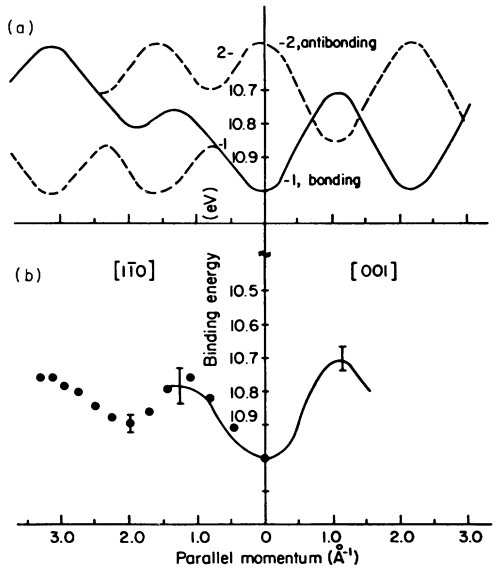

FIG. 11. (a) Band structure (dashed lines) and weighted mean peak position (solid line) for the 2×2 geometry of Fig. 10 in the plane-wave final-state approximation. Binding-energy scale is adjusted to fit the 4σ data below. (b) 4σ peak position. Solid line is the data of Fig. 9 and the circles are data from another sample taken at 70-eV photon energy at a 45° angle of incidence.

broadened while the 1×2 are merely weakened. Spot width is easily related to domain size.[29] The fact that no 2×2 spots are seen implies that the assumed 2×2 domains must be smaller than about 5 unit cells on a side, or include less than about 50 CO molecules.

To show how this geometry can explain the UPS data, the 4σ level has been chosen for a detailed comparison of data and prediction because it is well separated in binding energy from the other levels, and because it is not expected to mix with the substrate. The results found, if scaled to the 5σ bandwidth, should apply to the 5σ level as well, so long as metal and/or 1π hybridization can be ignored. The results of a parametrized tight-binding calculations with only nearest-neighbor interactions are presented for the 4σ-derived bands. No substrate interaction is included. Parametrized means that no overlap integrals are calculated, but that the binding-energy scale is adjusted for agreement with the data. The binding energy at $K=0$ is obtained directly from the data, and the bandwidth is adjusted to match the observed behavior of the 4σ band in the [001] direction. With the input of these parameters the band structure is plotted in Fig. 10(a) as dashed lines.

In the [001] direction band 1 is a simple bonding combination of the basis elements and band 2 is the antibonding combination. In the $[1\bar{1}0]$ direction these two combinations hybridize with an intermediate K-dependent phase $f(K)$ between the basis elements.

The two bands are separated by about 0.3 eV while each peak has an intrinsic width of about 0.9 eV. Thus the two bands are never resolved. What would be seen is a peak at some intermediate energy whose position depends on the relative intensities of the two bands. In the [001] direction these relative intensities are easy to calculate. The symmetry rules require zero intensity from the antibonding band 2. Thus band 1 is itself the weighted mean.

In $[1\bar{1}0]$, due to the hybridization of the bonding and antibonding combinations, symmetry rules are no help and the relative intensities must be explicitly calculated. The simplest approximation one can make is to assume a plane-wave final state. This approximation is clearly a poor one to make when calculating absolute cross sections for low photon energies. It is not, however, entirely unreasonable to hope that this approximation might be sufficient to determine the difference in emission intensities between these two very similar bands.

Most importantly, the application of this approximation yields a very simple answer. Gadzuk notes that the calculation of the matrix element in the plane-wave final-state approximation is equivalent to taking the Fourier transform (FT) of the initial-state wave function.[30] This is a very simple result which can be viewed as diffraction from the two basis elements. When the FT's are squared they yield, for the relative intensities from the two bands,

$$I_1(K)\propto\{1+\cos[f(K)-KB]\}\ ,$$
$$I_2(K)\propto\{1-\cos[f(K)-KB]\}\ . \tag{1}$$

B is the basis element spacing, 3.04 Å, and K is restricted to the $[1\bar{1}0]$ azimuth. These intensities are used to determine the mean peak positions which are plotted as solid lines in Fig. 11(a). These solid lines should be directly comparable with the observed 4σ peak motion of Fig. 11(b). These data are the data of sample 1 presented on an expanded scale, together with additional data taken on sample 2 at a photon energy of 70 eV.

There is substantial qualitative agreement between the calculated and observed peak motion. Most significantly, the predicted peak motion is now relatively isotropic, in agreement with the data. The major source of this agreement, which was qualitatively absent for the simple rectangle, is the generation of a peak in the E-vs-K curve at about 1.2 Å^{-1} in the $[1\bar{1}0]$ direction with an amplitude comparable to the [001] bandwidth. This peak is, loosely speaking, generated by intrabasis interference and not by the relatively flat band structure.

The effect of disorder on the UPS peak positions must still be considered. Two points make the UPS less sensitive to disorder than the LEED. The first point is that the binding energies are determined by nearest-neighbor interactions. Small domains put a coarse grid on the allowed energies but do not significantly affect their values. Second, the UPS peaks are inherently broad. This width defeats any attempt at discriminating between fine and coarse initial-state-energy grids (and thus between large and small domains). Peak motion for the disordered system is expected to be quite similar to that of the perfect 2×2, and still agree with the data.

VI. CONCLUSIONS

Angle-resolved UPS data from the CO-Fe(110) system have been presented and discussed. Normal-emission peak positions are summarized in Table I and the bandwidths observed appear in Table II. One of the interesting features observed was the large binding-energy separation of the 5σ and 1π levels. It was pointed out that this binding-energy separation might be an indication that the C—O bond has been stretched by 0.1 Å, which could be a precursor to the dissociation observed at room temperature. Another interesting feature was the

observed isotropy of the peak motion versus the parallel component of the final-state momentum. This is in marked contrast to the anisotropy of the geometry assumed on the basis of the LEED pattern. This discrepancy motivated the proposal of another more isotropic geometry that could also be made consistent with the LEED pattern. Within the plane-wave final-state approximation to UPS it was shown that this geometry could explain the observed peak motion. These two arguments represent attempts to infer adsorption geometry from angle-resolved UPS spectra. No direct evidence of either a stretched C—O bond or a distorted overlayer exists.

The 4σ and 5σ bandwidths observed in the [001] direction are about as large as predicted, and quite similar to those observed on other substrates.[21,22] The 1π peak is, however, surprisingly nondispersive. It was pointed out that this might be due to 1π hybridization with either the 5σ level or with the metal, although no specific mechanism was proposed. A simple overlap calculation for the model system linear-metal CO might verify either of these hypotheses. Many calculations of the orbital binding energies and wave functions for such systems have been done.[9–12]

ACKNOWLEDGMENTS

The Cornell research is supported by the Materials Science Center [National Science Foundation (NSF) Grant No. DMR-79-24008] of Cornell University. The synchrotron radiation work was done at the Synchrotron Radiation Center, Physical Sciences Laboratory, Stoughton, Wisconsin. We are grateful to E. M. Rowe, R. Otte, and the staff of the Tantalus I storage ring for making the facility available to us. Tantalus I is supported by the NSF under Grant No. DMR-77-21888 and the University of Wisconsin, Milwaukee, Graduate School. We are grateful for assistance from C. W. Seabury, L. G. Salmon, R. P. Merrill, and M. Cohen.

[1]E. Jensen, C. Seabury, and T. Rhodin, Solid State Commun. 35, 581 (1980).

[2]E. Jensen and T. Rhodin, J. Vac. Sci. Technol. 18, 470 (1981).

[3]C. Burris, J. Chem. Phys. 28, 427 (1958).

[4]A. Gaydon, *Dissociation Energies and Spectra of Diatomic Molecules* (Chapman and Hall, London, 1953).

[5]S. Andersson, Solid State Commun. 21, 75 (1977).

[6]C. Allyn, T. Gustafsson, and E. Plummer, Solid State Commun. 28, 85 (1978).

[7]S. Andersson and J. Pendry, Phys. Rev. Lett. 43, 363 (1979).

[8]M. Passler, A. Ignatiev, F. Jona, D. Jepsen, and P. Marcus, Phys. Rev. Lett. 43, 360 (1979).

[9]P. Bagus, K. Herman, and M. Seel, J. Vac. Sci. Technol. 18, 435 (1981); K. Herman and P. Bagus, Phys. Rev. B 16, 4195 (1977).

[10]D. Saddei, H. Freund, and G. Hohlneicher, Surf. Sci. 95, 527 (1980).

[11]G. Blyholder, J. Vac. Sci. Technol. 11, 865 (1974).

[12]L. Cederbaum, W. Domcke, W. von Hessen, and W. Brenig, Z. Phys. B 21, 381 (1975).

[13]H. Freund and E. Plummer, Phys. Rev. B 23, 4859 (1981).

[14]G. Brodén, G. Gafner, and H. Bonzel, Appl. Phys. 13, 33 (1977).

[15]G. Brodén, T. Rhodin, C. Brucker, R. Benbow, and Z. Hurych, Surf. Sci. 59, 593 (1976).

[16]J. Davenport, Phys. Rev. Lett. 36, 945 (1976); J. Davenport, Ph.D. thesis, University of Pennsylvania, 1976 (unpublished).

[17]I. Batra, K. Herman, A. Bradshaw, and K. Horn, Phys. Rev. B 20, 801 (1979).

[18]P. Larsen, N. Smith, M. Schluter, H. Farrel, K. Ho, and M. Cohen, Phys. Rev. B 17, 2612 (1978).

[19]K. Horn, A. Bradshaw, and K. Jacobi, Surf. Sci. 72, 719 (1978).

[20]K. Horn, A. Bradshaw, K. Herman, and I. Batra, Solid State Commun. 31, 257 (1979).

[21]C. Seabury, E. Jensen, and T. Rhodin, Solid State Commun. 37, 383 (1981).

[22]H. Freund, D. Hesket, and F. Greuter, reported in a review by E. Plumer and W. Eberhardt entitled *Angle Resolved Photoemission as a Tool for the Study of Surfaces,* Vol. 49 of *Advances in Chemical Physics,* edited by I. Prigogine and S. A. Rice (Wiley, New York, 1982).

[23]W. Erley, J. Vac. Sci. Technol. 18, 472 (1981).

[24]K. Jacobi, M. Scheffler, K. Kambe, and F. Forstman, Solid State Commun. 22, 17 (1977).

[25]C. W. Seabury, Ph.D. thesis, Cornell University, 1980 (unpublished).

[26]C. Allyn, T. Gustafsson, and W. Plummer, Solid State Commun. 24, 531 (1977).

[27]D. Turner, C. Baker, A. Baker, and C. Brundle, *Molecular Photoelectron Spectroscopy* (Wiley-Interscience, London, 1971).

[28]U. Gelius, E. Basilier, S. Svensson, T. Bergmark, and K.

Siegbahn, J. Electron. Spectrosc. Relat. Phenom. 2, 405 (1973).

[29]M. Henzler, in *Electron Spectroscopy for Surface Analysis,* edited by H. Ibach (Springer, New York, 1977).

[30]J. W. Gadzuk, Phys. Rev. B 10, 5030 (1974).